TEMPERATURE AND COMPOSITION DISTRIBUTIONS OF $LaNi_5H_6$ METAL HYDRIDE FOR DIFFERENT GEOMETRIES AND FLOW REGIMES IN HYDROGEN ENERGY CONDUCTION BED MODEL

M.A. El-Osairy
Dept. of Eng. Math. and Phys.,
Alexandria University,
Alexandria, Egypt.

I.A. El-Osery
Nuclear Power Plant Authority,
P.O. Box 108, Abbassia,
Cairo, Egypt.

A.M. Metwally
Nuclear Eng. Dept.,
Alexandria University,
Alexandria, Egypt.

Mayssa A. Hassan
Department of Eng. Math. and Phys.,
Alexandria University, Egypt.

ABSTRACT

Energy and mass balance equations, of metal hydrides for two dimensional hydrogen energy conduction bed model, were solved numerically by the use of the alternating direction implicit method. A computer code was applied to print out the temperature and metal hydride composition as well as the cumulative discharged hydrogen for different geometries and flow regimes. This work presents an evaluation study of different configurations for $LaNi_5H_6$ metal hydride storage beds with water as working fluid. Results have shown that; for the same operating conditions; the hydrogen discharging rate is the highest for the hollow cylindrical geometry with water passing inside the cylinder as well as the outer surface.

NOMENCLATURE

- A_f Wetted surface area of the cell (cm)
- C_f Fluid heat capacity (cal g^{-1} $^oC^{-1}$)
- C_s Solid heat capacity (cal g^{-1} $^oC^{-1}$)
- D_H Hydraulic Diameter (cm)
- H Height of the cell (cm)
- h Heat transfer coefficient (cal $^oC^{-1}$ cm^{-2} s^{-1})
- K Effective cell thermal conductivity (cal$^oC^{-1}$ cm^{-1} s^{-1})
- K_f Fluid thermal conductivity (cal $^oC^{-1}$ cm^{-1} s^{-1})
- M_w Molecular weight of metal hydride divided by number of metal atoms per molecule of hydride, [g $(g\ mole)^{-1}$]
- $\dot{m}$ Fluid mass flux (g s^{-1} cm^{-2})
- $\dot{m}_f$ Fluid mass flow rate (g s^{-1})
- Q Heat of reaction per unit hydrogen mass [cal$(gH_2)^{-1}$]
- R Reaction rate (g H_2 s^{-1} cm^{-3})
- r Radial distance (cm)
- T Solid temperature (°C)
- t Time (s)
- T_f Fluid temperature (^oC)
- z Axial distance (cm)
- ρ_s Solid density (g cm^{-3})
- ε Bed void fraction (free-to-total volume ratio)
- ξ Hydrogen-to-metal atom ratio (H/M)
- μ_f Fluid viscosity (g s^{-1} cm^{-1} or Poise)
- γ Geometric selection parameter equals 0 for rectangular plate or 1 for cylindrical geometry
- γ_1 Configuration selection parameter equals 0 for one-dimensional or 1 for two-dimensional problem

1. INTRODUCTION

Hydrogen can be stored as gas, liquid or metal hydrides. Hydrogen storage as metal hydrides is gaining more attention as it has the merits of high volumetric hydrogen density as well as safe handling and long term stability without refrigeration requirements [1,2].Two models have been developed for metal hydrides storage beds, namely the conduction bed model and the convection bed model, depending on the mode of heat transfer. In both models, hydrogen is discharged from the metal hydride through an endothermic chemical reaction. For metal hydrides used in energy storage applications, the conduction bed model is preferred due to its simplicity, safety considerations and the availability of using different fluids [3].

In a previous work [4], the problem of the discharging process associated with metal hydrides is solved analytically in space and time under certain simplifying assumptions encountered the process of physical and mathematical simulation. In the computer code "TOBAM" [5], the energy and mass heat transfer problems associated with metal hydride storage beds were solved numerically in two-dimensions through the use of the alternating direction implicit method [6]. The computer code has been carried out to solve the fluid energy equation and to allow for the variation of the fluid physical properties such as the thermal conductivity, specific heat and viscosity with the fluid operating temperature. The computer code gives as output the space-time temperature and metal hydride composition as well as the cumulative discharged hydrogen associated with different bed geometries and flow regimes.

This work presents the temperature and composition distributions of $LaNi_5H_6$ metal hydride, associated with the discharging process, for different geometries and flow regimes in two-dimensional hydrogen energy conduction bed model to obtain the optimum bed design and performance.

2. MATHEMATICAL MODEL

Physically, the hydrogen discharging process is modelled as endothermic chemical reaction.Considering fixed physical and operating conditions, the general formula of space-time dependent energy balance equation, for rectangular plate (or cylindrical) geometry, can be written as:

$$K\frac{\partial^2 T}{\partial r^2}+\frac{\gamma K}{r}\frac{\partial T}{\partial r}+\gamma_1 K\frac{\partial^2 T}{\partial z^2}-(1-\varepsilon)RQ=(1-\varepsilon)\rho_s C_s\frac{\partial T}{\partial t} \quad (1)$$

and the associated mass balance equation is given as:

$$\frac{\partial \xi}{\partial t}=-\frac{M_w}{\rho_s}R \quad (2)$$

where "R" is the reaction rate which is considered linearly dependent on the hydrogen fraction being completely reacted and the hydrogen pressure, while it is considered exponentionally dependent on the hydride temperature. Thus, it can be represented as :

$$R=f_1(\xi,P,T)=\frac{\xi-\xi_F}{\xi_I-\xi_F}*\frac{P_D-P_b}{P_D}*A_1\exp\left[\frac{-A_2}{T+273}\right] \quad (3)$$

where

$$P_D=f_2(T)=\exp\left[\frac{A}{T+273}+B\right] \quad (4)$$

and A_1, A_2, A and B are metal hydride specific constants.

The energy and mass balance equations are to be solved under the initial conditions :

$$\begin{aligned} T(r,z,0)&=T_I \\ \xi(r,z,0)&=\xi_I \end{aligned} \quad (5)$$

for $r_i \le r \le r_o$ and $0 \le z \le H$.

The associated boundary conditions for the CCTT-alternative are [4]:

$$\begin{aligned} K\frac{\partial T}{\partial r}&=\alpha_1 h_i[T-T_{fi}] \quad ; \quad r=r_i \\ K\frac{\partial T}{\partial r}&=-\alpha_2 h_o[T-T_{fo}] \quad ; \quad r=r_o \\ T&=T_{fI} \quad ; \quad z=0 \\ T&=T_{fE} \quad ; \quad z=H \end{aligned} \quad (6)$$

The energy balance equation for the fluid can be written as [8]:

$$\frac{\dot{m}_f C_f H}{h A_f}\frac{\partial T_f}{\partial z}=T-T_f \quad (7)$$

and the heat transfer coefficient can be calculated using the correlation[3] :

$$h=\left[\frac{0.023\ K_f}{D_H}\right]\left[\frac{D_H \dot{m}}{\mu_f}\right]^{0.8}\left[\frac{\mu_f C_f}{K_f}\right]^{0.4} \quad (8)$$

The first step of the numerical solution is to transfer the mathematical formulation into a dimensionless form. Then a discrete form of the problem is developed using the alternating direction implicit (ADI) method [6]. The main idea in this method is to use two difference equations successively through which the time step is always half the time increment. There will be two finite difference equations for energy balance equation, the first is implicit only in the radial direction (X-direction) while the second is implicit only in the axial direction (Y-direction). The numerical solution of the problem gives the space-time nodal values of the temperature, the

hydrogen-to-metal atom ratio (H/M) and the cumulative discharged hydrogen [5].

3. REFERENCE MODEL

The reference conduction bed model is composed of a multiple of hollow cylindrical or rectangular plate cells of the metal hydride. There is a thin conducting wall between the metal hydride and the heating fluid, so the temperature gradient across it can be considered zero. The computer code is applied to the CCTT boundary conditions alternative given in equation (6). In this case the lower surface of the bed is maintained at constant inlet fluid temperature and the upper surface is maintained at constant temperature corresponding to the exit fluid temperature. In this alternative either convective boundary conditions or insulated boundary conditions are applied to the inner and outer surfaces according to the cell geometry and its flow regime which can be one of the following:

1. Rectangular plate (P) : in which fluid flows, in the Y-direction, over the two opposite sides of a rectangular plate.
2. Cylinder (CI) : in which the fluid flows inside the cell while the outer surface is insulated.
3. Cylinder (CO) : in which the fluid flows over the outer surface of the cell while its inner surface is insulated.
4. Cylinder (CIO) : in which the fluid flows over both, the inner and the outer surfaces of the cell.

In order to have common bases for comparison between the cylindrical and the rectangular plate cell geometries, it is assumed that the contained volume of the metal hydride in each cell is constant and is equivalent to the volume of a sphere of radius 10 cm. The inner and outer radii of the cylindrical geometry were selected to be 1 and 11 cm respectively, and the thickness and height of the rectangular plate geometry were selected to be 20 and 10 cm respectively. The cylinder height and the rectangular plate width were adjusted by the code to yield the constant volume.

Table (1) shows the physical and operating conditions for all the cell alternatives. The physical properties of $LaNi_5H_6$ metal hydride are referred to reference [9].

Table 1. Physical and operating conditions of $LaNi_5H_6$

Parameter	Value
Bed effective thermal conductivity, cal./cm sec °C	0.003152
Solid heat capacity, cal./gm °C	0.1366
Solid density, gm/cm^3	6.59
Heat of reaction per unit mass of hydrogen, cal./gm H_2	3701.94
Molecular weight of metal hydride, gm/ gm mole	438.4
Bed void fraction	0.4
Bed hydrogen pressure, atm.	1.0
Initial bed temperature, °C	10.0
Inlet fluid temperature, °C	80.0
Initial hydrogen-to-metal atom ratio $(H/M)_I$	1.0
Final hydrogen-to-metal atom ratio $(H/M)_F$	0.05
Water mass flux, gm/ cm^2 sec	10.0

4.RESULTS AND DISCUSSIONS

The computer code "TOBAM" is used to study and analyze the process of discharging hydrogen from $LaNi_5H_6$ metal hydride storage bed using water as a heat transfer fluid. The obtained results are presented in Figures (1) through (9).

Figures (1-4) present the dimensionless radial temperature distributions at 90 minutes discharging time and at different dimensionless axial distances for P, CI, CO, and CIO flow regimes respectively. From these figures, it is noticed that the temperature profiles have the concave shape due to the endothermic reaction associated with the dehydriding process. The radial temperature is maximum at the down surface of the cell (Y=0.0) since it equals the inlet fluid temperature. Figure (1) and Figure (3) show that for both P and CO flow regimes the maximum axial temperature profiles occur at the outer surface (X=1), where it is in a direct contact with the heating fluid. For the CI flow regime, it is noticed from Figure (2) that the maximum axial temperature profiles

occur at the inner surface (X=0.0), where it is in a direct contact with the heating fluid, while the minimum axial temperature profiles occur at the outer surface (X=1), where it is insulated boundary. For CIO flow regime, Figure (4) shows that the axial temperature is maximum at the inner and the outer surfaces (X=0.0 , X=1) where the heating fluid is in a direct contact with these surfaces. The radial temperature distributions are asymmetrical (minimum at about X=0.4) due to the fact that the heat transfer areas perpendicular to the radius are not equal.

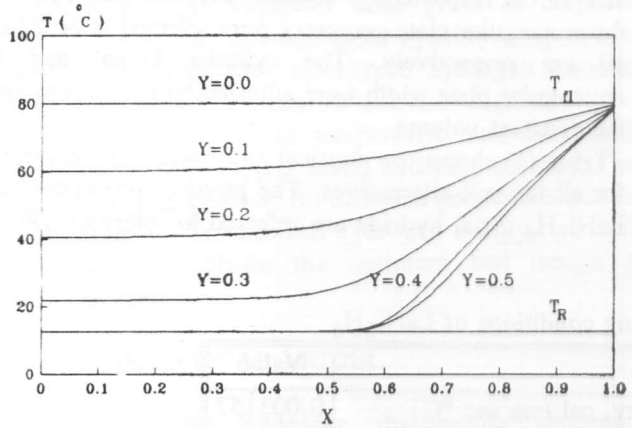

Figure 1. The dimensionless spatial temperature profiles at 90 minutes discharging time and at different dimensionless axial distances for P flow regime.

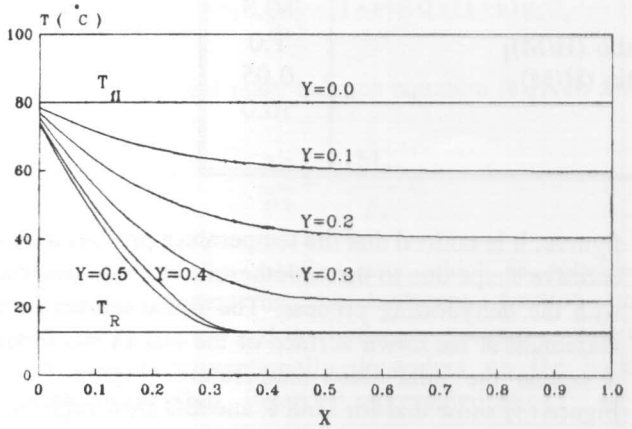

Figure 2. The dimensionless radial temperature profiles at 90 minutes discharging time and at different dimensionless axial distances for CI flow regime.

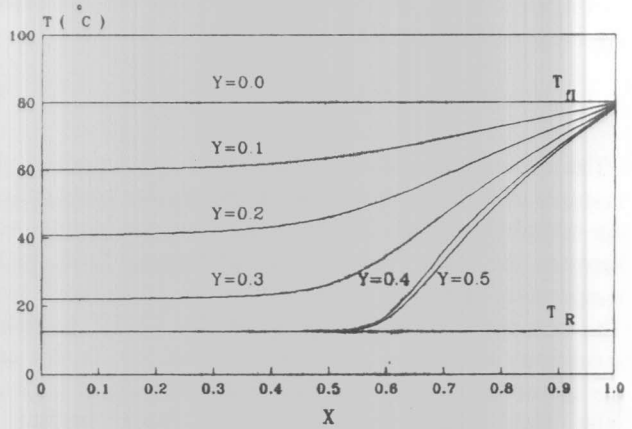

Figure 3. The dimensionless radial temperature profiles at 90 minutes discharging time and at different dimensionless axial distances for CO flow regime.

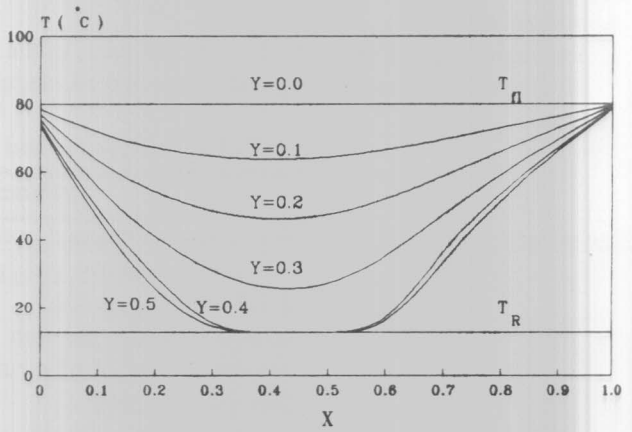

Figure 4. The dimensionless radial temperature profiles at 90 minutes discharging time and at different dimensionless axial distances for CIO flow regime.

Figures (5) - (8) illustrate the radial behaviour of hydrogen-to-metal atom ratio (H/M) at mid axial plane (Y=0.5) and at different discharging time progress associated with P, CI, CO and CIO flow regimes respectively. From these figures, it can be noticed that the sequence of hydrogen liberation from the radial locations are matched well with the heat transfer rate into the cell. This means that, the outer surface of P and CO flow regimes is the most effective location to liberate hydrogen, while the inner surface of the CI flow regime is the most effective location to liberate hydrogen. For CIO flow regime, hydrogen is liberated sequentially from the radial locations which are close to the outer and the inner surfaces.

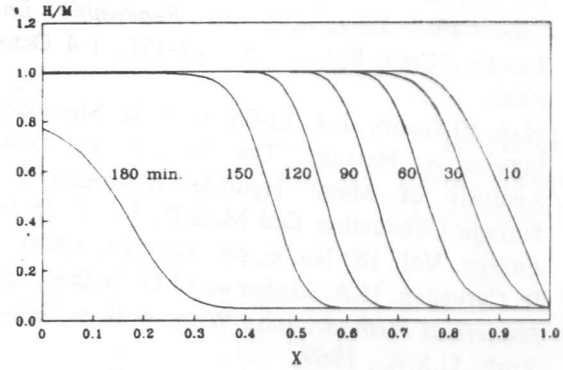

Figure 5. The dimensionless spatial behavior of hydrogen-to-metal atom ratio (H/M) at mid axial plane (Y=0.5) and at different discharging time associated with P flow regime.

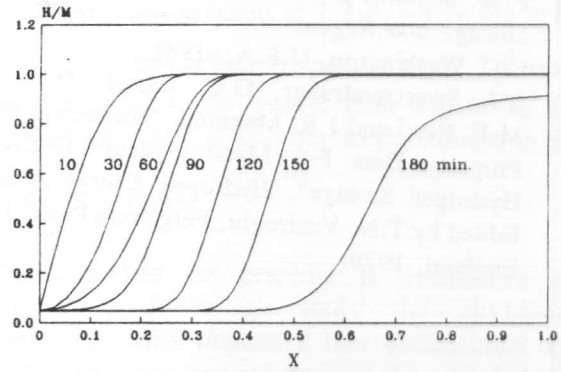

Figure 6. The dimensionless radial behavior of hydrogen-to-metal atom ratio (H/M) at mid axial plane (Y=0.5) and at different discharging time associated with CI flow regime.

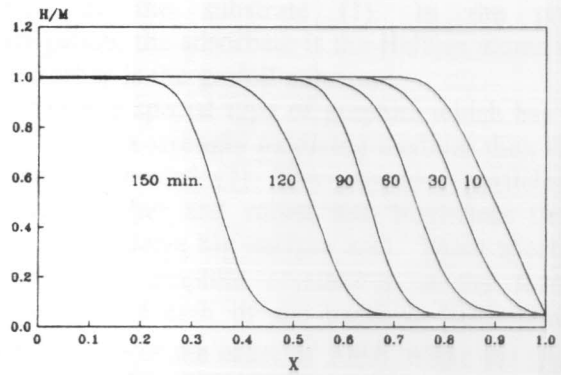

Figure 7. The dimensionless radial behavior of hydrogen-to-metal atom ratio (H/M) at mid axial plane (Y=0.5) and at different discharging time associated with CO flow regime.

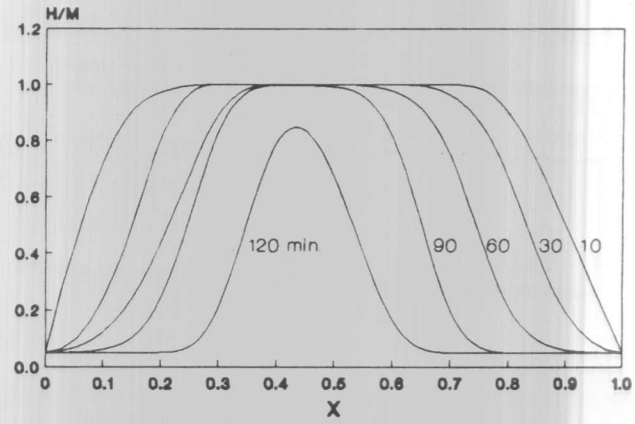

Figure 8. The dimensionless radial behavior of hydrogen-to-metal atom ratio (H/M) at mid axial plane (Y=0.5) and at different discharging time associated with CIO flow regime.

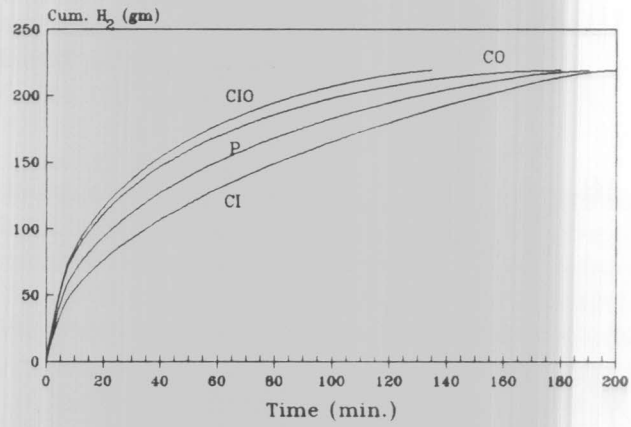

Figure 9. Time behavior of the cumulative discharged hydrogen in grams for different geometries and flow regimes.

Figure (9) illustrates the time behaviour of the cumulative discharged hydrogen for different geometries and flow regimes. Table (2) shows the cumulative discharged hydrogen at 90 minutes of the discharged time and the termination time of the discharging process for different flow regimes. The values given in percent express the cumulative hydrogen in percent of the total hydrogen content in the metal hydride contained in the storage cell. It can be concluded that for the same operating conditions, the rate of hydrogen discharge is the highest when using the CIO flow regime while it is the lowest for CI flow regime.

Table 2. Comparison of the cumulative discharged hydrogen for the different flow regimes.

Flow regime	Cumulative H_2, at 90 min., gm	Termination time, min.
P	176 , [80.4%]	192
CI	157 , [71.7%]	199
CO	192 , [87.7%]	181
CIO	201.5 , [92.0%]	136

REFERENCES

[1] D.P. Gregory, "The Role of Hydrogen in The Energy Future of The United States", *Int. J. Hydrogen Energy*, Vol. 1, pp. 109-112, Pergamon Press, 1976.

[2] I.A. El-Osery, "A Nuclear-Electric-Hydrogen-Energy System", *Energy Journal* (Oxford), Vol. 9, pp. 709-711, U.K., 1984.

[3] W.S. Yu, E. Suuberg, and C. Waide, "Modelling Studies of Fixed-Bed Metal Hydride Storage Systems", *in Hydrogen Energy (Part A)*, Edited by T.N. Veziroglu, Plenum Press, pp. 621-643, New York, U.S.A., 1975.

[4] I.A.El-Osery, A.M. Metwally, M.A. El-Osairy and Mayssa A. Hassan, "Toward an Analytical Solution for Heat Transfer Problems in Metal Hydride Conduction Bed Model", *Proceedings of The Second Cairo Int. Symposium on Renewable Energy Sources*, Cairo-Egypt, pp. 443-451, 1-4 October, 1990.

[5] M.A. El-Osairy, I.A. El-Osery, A.M. Metwally and Mayssa A. Hassan, "Two Dimensional Dynamic Analysis of Metal Hydride Hydrogen Energy Storage Conduction Bed Model", *Int. J. Hydrogen Energy*, Vol. 18, No. 6, pp. 517-524, 1993.

[6] B. Carnahan, H.A. Luther and J.O. Wilkes, *Applied Numerical Methods*, John Wiley & Sons Inc., New York, U.S.A., 1969.

[7] I.A. El-Osery, "Theory of The Computer Code RET1 For The Calculation of Space-Time Dependent Temperature and Composition Properties of Metal Hydride Hydrogen Storage Beds", *Int. J. Hydrogen Energy*, Vol. 81, pp. 191-198, 1983.

[8] F.W. Schmidt and A.J. Willmott, *Thermal Energy Storage and Regeneration*, Hemisphere Publishing Co., Washington, U.S.A., 1981.

[9] L.J. Swartzendruber, G.C. Carter, D.J. Kahan, M.E. Read and J.R. Manning, "Numerical Physical Property Data For Metal Hydride Utilized For Hydrogen Storage", *Hydrogen Energy System IV*, Edited by T.N. Veziroglu, Pergamon Press, Oxford, England, 1979.